PHYSICAL REVIEW B, VOLUME 65, 201301(R)

Spin instabilities and quantum phase transitions in integral and fractional quantum Hall states

Arkadiusz Wójs[1,2] and John J. Quinn[1]
[1]Department of Physics, University of Tennessee, Knoxville, Tennessee 37996
[2]Institute of Physics, Wroclaw University of Technology, Wroclaw 50-370, Poland

(Received 5 February 2002; published 22 April 2002)

The spin excitations of quantum Hall states at filling factors $\nu=2$ and $\frac{4}{3}$ are investigated numerically in the systems with comparable cyclotron ($\hbar\omega_c$) and Zeeman (E_Z) gaps. The relevant quasiparticles and their interactions are studied, including spin wave and skyrmion bound states. For $\nu=2$, a spin instability at a finite value of $\varepsilon=\hbar\omega_c-E_Z$ leads to an abrupt paramagnetic to ferromagnetic transition, in agreement with the mean-field approximation. However, for $\nu=\frac{4}{3}$ a new quantum phase transition is found in finite-size droplets that involves a gradual change from para- to ferromagnetic occupancy.

DOI: 10.1103/PhysRevB.65.201301 PACS number(s): 73.43.Nq, 73.21.−b, 75.30.Fv

The elementary excitations of a two-dimensional electron gas (2DEG) with energy quantized into Landau levels (LL's) by a high magnetic field B have been extensively studied for decades. The charge excitations govern transport, including the integral and fractional quantum Hall effects (IQHE and FQHE).[1] The spin excitations appear in the context of spin waves (SW's),[2] spin instabilities, related quantum phase transitions (QPT's),[3,4] and skyrmions.[5,6]

In this Rapid Communication we study spin excitations of IQH and FQH systems with densities ϱ corresponding to the filling factors $\nu=2\pi\varrho\lambda^2\approx 2$ and $\frac{4}{3}$ (here, $\lambda=\sqrt{\hbar c/eB}$ is the magnetic length). The cyclotron ($\hbar\omega_c$) and Zeeman (E_Z) splittings are assumed comparable and much larger than the Coulomb energy $E_C=e^2/\lambda$. In this situation, the spin excitations couple two partially filled LL's with different orbital indices, $n=0$ and 1. These LL's, denoted by $|0\uparrow\rangle$ and $|1\downarrow\rangle$, are separated by a small gap $\varepsilon=\hbar\omega_c-E_Z\ll E_C$ from each other and by large gaps $\sim\hbar\omega_c\gg E_C$ from the lower, filled $|0\downarrow\rangle$ LL and from the higher, empty LL's, as shown schematically in Fig. 1(c).

For the $\nu=2$ ground state (GS), it is well known[3] that a spin-flip instability occurs at a finite gap ε and wave vector k. In the mean-field approximation (MFA), this instability signals an abrupt, interaction-induced QPT from paramagnetic (P;$|0\downarrow\rangle$ and $|0\uparrow\rangle$ filled) to ferromagnetic (F;$|0\downarrow\rangle$ and $|1\downarrow\rangle$ filled) occupancy. Our numerical results confirm the validity of the MFA for $\nu=2$. However, for $\nu=\frac{4}{3}$ they predict a new and unexpected $P\rightarrow F$ QPT that occurs through a series of intermediate GS's with increasing number of spin flips as ε is decreased from ε_P to ε_F (the lower and upper boundaries of ε for the P and F occupancies, respectively). Since the transition range $\Delta\varepsilon=\varepsilon_P-\varepsilon_F$ scales with the inverse system size, the gradual $P\rightarrow F$ QPT should be experimentally observed only in finite FQH droplets.[7]

The model is the same as that used earlier,[6,8] except that now the spin excitations connect two different LL's. The electrons are confined to a spherical surface[9] of radius R. The radial magnetic field B is due to a monopole of strength $2Q$, defined in units of the flux quantum $\phi_0=hc/e$ so that $4\pi R^2B=2Q\phi_0$ and $R^2=Q\lambda^2$. The single-electron states are labeled by angular momentum $l=Q+n$ and its projection m.

Only the partially filled $|0\uparrow\rangle$ and $|1\downarrow\rangle$ LL's (labeled by pseudospin $s=\uparrow$ and $\downarrow$) are included in the calculation, and the filled, rigid $|0\downarrow\rangle$ LL enters through the exchange energy Σ_{10}. The ratio ε/E_C is taken as an arbitrary parameter. Although we do not discuss the effect of the finite width w of a realistic 2DEG (Ref. 6) and only present the results obtained using the pseudopotential $V(\mathcal{R})$ (interaction energy as a function of relative pair angular momentum[10]) for $w=0$, shown in Fig. 1(a), we have checked that our conclusions remain valid for $w\leqslant 5\lambda$.

The Hamiltonian H for electrons confined to the $|0\uparrow\rangle$ and $|1\downarrow\rangle$ LL's contains the single-particle term ($\varepsilon-\Sigma_{10}$) and the intra- and inter-LL two-body interaction matrix elements $\langle m_1s,m_2s'|V|m_3s',m_4s\rangle$ calculated for the Coulomb potential $V(r)=e^2/r$ and connected with pseudopotentials $V_{ss'}(\mathcal{R})$ shown in Fig. 1(a) through the Clebsch-Gordan coefficients (on a sphere, $\mathcal{R}=2l-L$ where $L=\mathbf{l}_1+\mathbf{l}_2$ is pair angular momentum).

Hamiltonian H is diagonalized in the basis of N-electron Slater determinants $|m_1s_1\cdots m_Ns_N\rangle$. This allows automatic resolution of the projection of pseudospin ($S_z=\Sigma s_i$) and of angular momentum ($L_z=\Sigma m_i$). The quantum number $K=\frac{1}{2}N+S_z$ measures the number of reversed spins relative to the paramagnetic configuration. The length of angular momentum (L) is resolved numerically in the diagonalization of each (S_z,L_z) Hilbert subspace. The length of pseudospin is not a good quantum number because of the pseudospin-asymmeteric interactions. The results obtained on Haldane sphere are easily converted to the planar geometry, where L and L_z are appropriately[11] replaced by the total and center-of-mass angular momentum projections, M and $M_{\rm CM}$.

Let us begin with the discussion of the IQH regime. Figure 2 presents the spin-excitation spectra for $N=14$, at the filling factors equal to or different by one flux from $\nu=2$. Only the lowest state is shown for each K and L. The energy E is measured from the lowest paramagnetic state (at $E=E_0$) and excludes the inter-LL gap ε. Symbols e^* and h denote reversed-spin electrons (particles in the $|1\downarrow\rangle$ LL) and holes (vacancies in the $|0\uparrow\rangle$ LL) created in the "vacuum" state (completely filled $|0\uparrow\rangle$ LL).

The excitation spectrum of the "vacuum" state is shown in Fig. 2(b). The $K=1$ band is a SW; in a finite system it has $L=1$ to N, as follows from addition of the e^* and h angular momenta, $l_{e^*}=Q+1$ and $l_h=Q$. In an infinite system, the

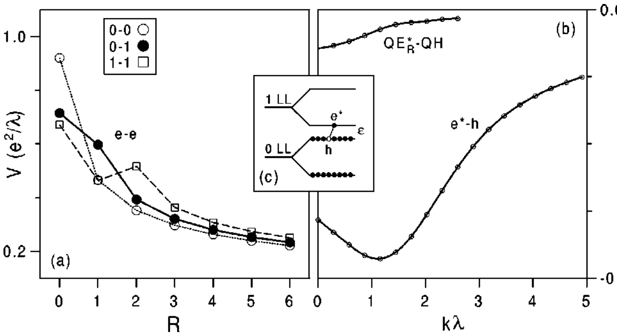

FIG. 1. The Coulomb pseudopotentials V for the pair of (a) electrons in the $n=0$ and 1 LL's, and (b) reversed-spin electron (e^*) or quasielectron (QE_R^*) in the $n=1$ LL and hole (h) or quasihole (QH) in the $n=0$ LL. (c) Schematic of the LL structure at $\nu=2$, with the h and e^* quasiparticles.

continuous SW dispersion is given by[2] $E_{\mathrm{SW}}(k)=E_0+\frac{1}{2}E_{\mathrm{C}}\sqrt{\pi/2}\{1-\exp(-\kappa^2)[(1+2\kappa^2)I_0(\kappa^2)-2\kappa^2I_1(\kappa^2)]\}$, where $\kappa=\frac{1}{2}k\lambda$, I_0 and I_1 are the modified Bessel functions, and $k=L/R$. $E_{\mathrm{SW}}(k)$ starts at $E=E_0$ for $k=0$ and has a minimum at $k\approx1.19\lambda^{-1}$ and $E\approx E_0-0.147\ E_C$. The vanishing of SW energy at $k=0$ is the result of exact cancellation of the sum of e^* and h exchange self-energies, $-\Sigma_{10}+\Sigma_{00}$, by the e^*–h attraction V_{e*h} at $k=0$; the entire e^*–h pseudopotential is shown in Fig. 1(b).

The energy spectra corresponding to consecutive spin flips ($K=2,3,\dots$) at $\nu=2$ all contain low-energy bands at $L\geqslant K$. For each K, the GS's (open circles) have $L=K$ and their energies fall on a nearly straight line, $E(K)$. These GS's are therefore denoted by $\mathcal{W}_K=K\times\mathrm{SW}$ and interpreted as containing K SW's with parallel angular momenta each of length $L=1$, similar to the $L=K$ SW condensates at $\nu=1$.[6] The new feature at $\nu=2$ is the SW-SW attraction (due to a finite dipole moment of an inter-LL SW) giving rise to a negative slope of $E(K)$.

Let us now turn to Figs. 2(a) and 2(c) showing spin excitation spectra in the presence of an e^* or h. The series of GS's for $K\geqslant1$ (open circles) are charged bound states, similar to the skyrmions and anti-skyrmions at $\nu=1$. Their angular momenta result from a simple vector addition of l_{e*} and l_h. For $\mathcal{S}_K^-=K\times\mathrm{SW}+e^*$ and $\mathcal{S}_K^+=K\times\mathrm{SW}+h$ we get $L=(\mathbf{l}_{e*})^{K+1}\oplus(\mathbf{l}_h)^K=Q+1$ and $L=(\mathbf{l}_{e*})^K\oplus(\mathbf{l}_h)^{K+1}=|Q-2K|$, respectively. In both cases, finite $L\propto Q$ means massive LL degeneracy, as expected for charged particles in a magnetic field.

Let us check if the negative SW energy at $k\approx1.19\lambda^{-1}$ or the SW-SW attraction causes instability of the $\nu=2$ GS towards the formation of one or more SW's when ε is decreased. The single-SW instability has been ruled out by Giuliani and Quinn[3] who showed that it is pre-empted by a direct transition to the ferromagnetic GS. The critical value of ε for this $P\rightarrow F$ QPT is expressed through the involved self-energies, $\varepsilon_0=\Sigma_{10}+\frac{1}{2}(\Sigma_{11}-\Sigma_{00})=\frac{3}{8}\sqrt{\pi/2}E_{\mathrm{C}}\approx0.47E_{\mathrm{C}}$, and it is larger than E_0-E_{SW}. Since the energy per spin flip, $[E(K)-E_0]/K$, is smaller for the SW condensates and skyrmions than for a single SW, we still need to check for a possible vac$\rightarrow\mathcal{W}_K$, $e^*\rightarrow\mathcal{S}_K^-$, or $h\rightarrow\mathcal{S}_K^+$ instability. Figure 3(a) shows that despite evident SW-SW, SW-e^*, and SW-h attraction ($\delta E=E-E_0+K\varepsilon_0$ is the energy to create K SW's in "vacuum" or in the presence of an e^* or h), the $\mathcal{W}_K$ and $\mathcal{S}_K^\pm$ energies are all positive at $\varepsilon=\varepsilon_0$. This precludes spin instability at $\nu=2$ other than the direct $P\rightarrow F$ transition (skipping the states with intermediate spin).

To translate our finite-size spectra to the case of an infinite 2DEG, in Fig. 3(b) we have plotted the energies of the SW condensate calculated for different electron numbers, $N\leqslant14$. Clearly, all data fall on the same curve when $\delta E/\sqrt{N}$ is plotted as a function of "relative" spin polarization, $\zeta=K/N$. This resembles the insensitivity to N of the $\delta E(\zeta)$ curves for the SW condensates at $\nu=1$, except that now $\delta E\propto N^{1/2}$ (rather than $\propto N^0$).

The data of Fig. 3 allow calculation of the SW binding energies, $U_K=[E(K-1)-E_0]+[E_{\mathrm{SW}}-E_0]-[E(K)-E_0]$, for the $\mathcal{W}_K$ and $\mathcal{S}_K^\pm$ states. Because of the SW-SW attraction, all these energies increase in a similar way as a function of K, in contrast to $\nu=1$ where U_K decreased for skyrmions and vanished for the SW condensate.

Let us now turn to the FQH regime. At $\nu=4/3$, which occurs for $2Q=3(N-1)$, and for sufficiently large ε, the N electrons in the $|0\uparrow\rangle$ LL form the Laughlin $\nu=\frac{1}{3}$ state. These electrons, each with angular momentum $l=Q$, can be converted into an equal number of composite fermions (CF's) (Ref. 12) each with effective angular momentum $l^*=l-(N-1)$, exactly filling their effective LL. The elementary

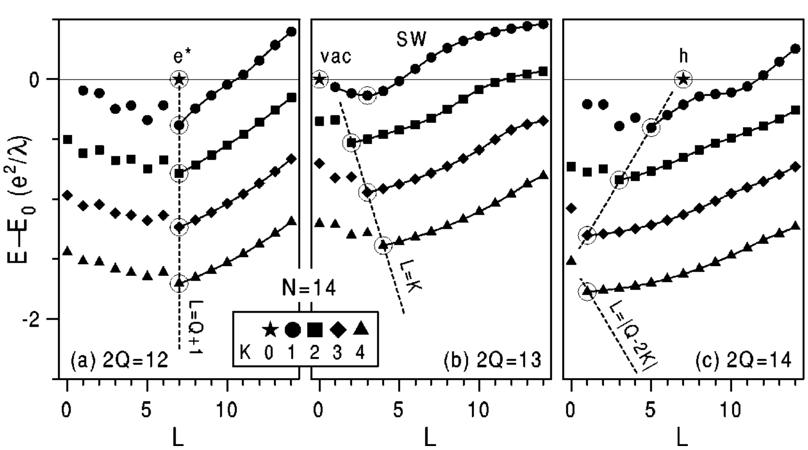

FIG. 2. The excitation energy spectra of 14 electrons in the $|0\uparrow\rangle$ and $|1\downarrow\rangle$ LL's calculated on a sphere for $2Q=12$ (a), 13 (b), and 14 (c), corresponding to filling factors $\nu\approx2$. The lowest $|0\downarrow\rangle$ LL is filled. E_0 is the energy of the lowest paramagnetic ($K=0$) state, and dashed lines mark the lowest states for different values of K.

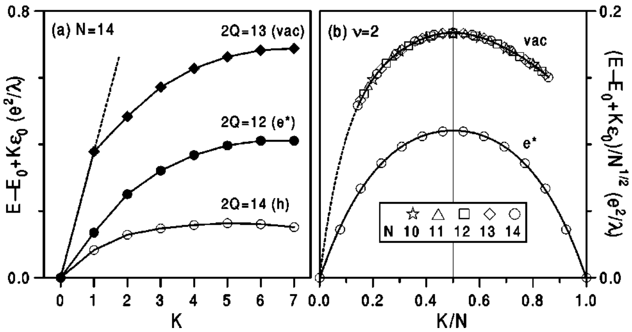

FIG. 3. (a) The energy of skyrmions, anti-skyrmions, and spin-wave condensates of Fig. 2, plotted as a function of K. Setting $\varepsilon=\varepsilon_0$ ensures degeneracy of para- and ferromagnetic ($K=0$ and N) configurations. (b) The energy of spin-wave condensates for $N=10$ to 14 (rescaled by $\sqrt{N}$) as a function of $\zeta=K/N$. The skyrmion curve is shown for comparison.

charge excitations of the $\nu=\frac{1}{3}$ state are two types of Laughlin quasiparticles (QP's), quasielectrons (QE's) and quasiholes (QH's), corresponding to an excess particle in an (empty) excited CF LL, or a hole in the (filled) lowest CF LL, respectively.

The reversed-spin quasielectrons (QE_R's) (Refs. 8 and 13) do not occur at $\nu=\frac{4}{3}$ because of the electrons completely filling the $|0\downarrow\rangle$ LL. This causes a difference between the SW's at $\nu=\frac{4}{3}$ and $\frac{1}{3}$, similar to that between $\nu=2$ and 1. At $\nu=\frac{1}{3}$ the SW consisted of a QH and a QE_R, and at $\nu=\frac{4}{3}$ it is formed by a QH and a different reversed-spin QP that we will denote by QE_R^*.

The QE_R^* has the same electric charge of $-\frac{1}{3}e$ as QE or QE_R but it belongs to an excited electron LL, $|1\downarrow\rangle$. Similar to the case for QH, QE, and QE_R, the existence and stability of the QE_R^* depend on the validity of the CF transformation for the underlying system of $N-1$ electrons in the $|0\uparrow\rangle$ LL and one electron in the $|1\downarrow\rangle$ LL. This requires Laughlin correlations between the $|1\downarrow\rangle$ electron and the $|0\uparrow\rangle$ electrons, i.e., the occurrence of a Jastrow prefactor, $\Pi_{ij}(z_i^{(0)}-z_j^{(1)})^{\mu}$, in the many-body wave function, with $\mu=2$ for $\nu=(1+\mu)^{-1}=\frac{1}{3}$. Such correlations result from short-range e–e repulsion, and the criterion is[14,15] that the pseudopotential V must decrease more quickly than linearly as a function of the average square e–e separation $\langle r^2\rangle$. On a plane (or on a sphere for $\langle r^2\rangle\ll R^2$, i.e., for $\mathcal{R}\ll Q$) this is equivalent to a superlinear decrease of V as a function of $\mathcal{R}$.

It is clear from Fig. 1(a) that the Coulomb inter-LL pseudopotential $V_{01}(\mathcal{R})$ is a short-range repulsion for $\mathcal{R}\geqslant\mathcal{R}_0=1$. This implies the Jastrow prefactors with $\mu>\mathcal{R}_0=2,3,\ldots$ in the $|0\uparrow\rangle^{N-1}\oplus|1\downarrow\rangle$ wave function, if only $\nu\leqslant(1+\mu)^{-1}$. In particular, this establishes the QE_R^* as a stable reversed-spin QP of the $\nu=\frac{4}{3}$ state, in analogy to the reversed-spin electron, e^*, at $\nu=2$. The angular momentum of QE_R^* on a sphere can be obtained in the two-component CF picture[16] appropriate for $\nu=\frac{1}{3}$, i.e., with both 0–0 and 0–1 Laughlin correlations modeled by attachment of two flux quanta to each electron. The resulting CF angular momenta are $l_{\mathrm{QH}}=Q^*$ and $l_{\mathrm{QE}}=l_{\mathrm{QE}_R^*}=Q^*+1$, where $Q^*=Q-(N-1)$.

The excitation spectra at filling factors equal to or different by one flux from $\nu=\frac{4}{3}$ are displayed in Fig. 4. $N=8$ in each frame, and the values of $2Q$ are 20, 21, and 22, corresponding to the following GS's at $K=0$: (a) QE at $L=4$, (b) "vacuum" (filled CF LL) with $L=0$, and (c) QH at $L=4$. The low-energy charge excitations for $2Q=21$ form the magnetoroton (QE+QH) band. The low-energy spin excitations with $K=1$ are the following: (a) QE_R^* at $L=l_{\mathrm{QE}_R^*}=4$ for $2Q=20$, (b) the SW ($\mathrm{QE}_R^*+\mathrm{QH}$) band with L going from 1 to $N=8$, as follows from vector addition of l_{QH} and $l_{\mathrm{QE}_R^*}$, for $2Q=21$, and (c) a band of $\mathrm{QE}_R^*+\mathrm{QH}_2$ states with a bound GS denoted as $\mathrm{QE}_R^*\mathrm{QH}_2$ for $2Q=22$.

To draw analogy with Fig. 2, QE corresponds to an electron in the $|1\uparrow\rangle$ LL (not shown because of high energy), QE_R^* to e^*, QH to h, and $\mathrm{QE}_R^*\mathrm{QH}_2$ to $\mathcal{S}_1^+$. The latter state is the only "skyrmion" at $\nu=\frac{4}{3}$. The $\mathcal{S}_K^-$ states with $K\geqslant1$ and $L=Q^*+1$ or the $\mathcal{S}_K^+$ states with $K\geqslant2$ and $L=|Q^*-2K|$ do not occur because of the weakened Coulomb repulsion at short range in the excited LL. As shown in Fig. 1(a), the linear behavior of $V_{11}(\mathcal{R})$ between $\mathcal{R}=1$ and 5 prevents Laughlin correlations for two or more electrons in the $n=1$ LL. This invalidates the CF model and causes breakup of QE_R^*'s when two of them approach each other (at this point, pairing of electrons in the $n=1$ LL occurs.[15,17]) For the same reason, no $\mathcal{W}_K$ states at $L=K$ appear in Fig. 4(b) for $K>1$.

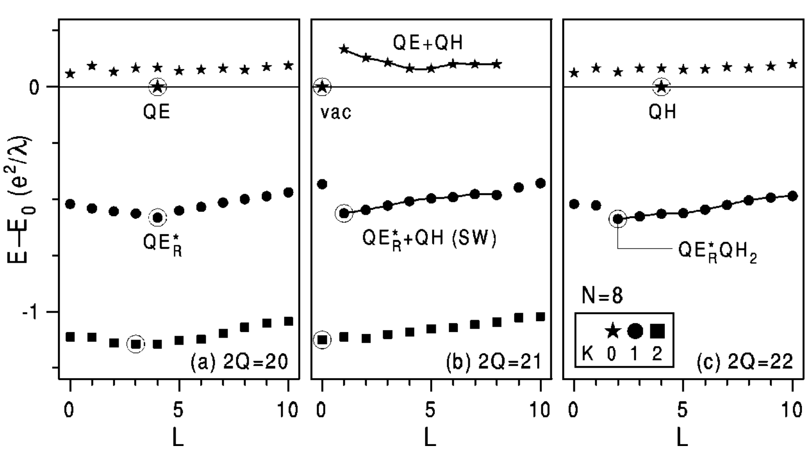

FIG. 4. Same as Fig. 2, but for $N=8$ electrons and for the monopole strengths $2Q=20$ (a), 21 (b), and 22 (c), corresponding to the filling factors $\nu\approx\frac{4}{3}$.

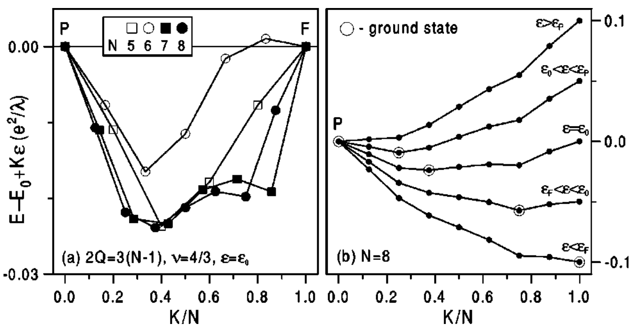

FIG. 5. (a) Same as Fig. 3(b), but for the filling factor $\nu=\frac{4}{3}$. (b) Data for $N=8$ plotted for different values of ε.

Even more significant in Fig. 4 than the absence of $\mathcal{S}_K^{\pm}$ and $\mathcal{W}_K$ states is the large and negative SW energy $E_{\rm SW}^*(k)$ at $\nu=\frac{4}{3}$. This is in striking contrast to the $\nu=2$ case, and it is explained as follows. The SW energy is the sum of the QE_R^* and QH self-energies and the QE_R^*–QH attraction. Of these three terms, only the QE_R^* self-energy, $-\Sigma_{10}=-\frac{1}{2}\sqrt{\pi/2}E_{\rm C}$, is the same at $\nu=2$ and $\frac{4}{3}$, while the QH self-energy Σ_{00}^* and the QE_R^*–QH pseudopotential $V_{\mathrm{QE}_R^*\mathrm{QH}}(k)$ are both reduced (because of only partial filling of the $|0\uparrow\rangle$ LL and the fractional QP charge, respectively). As a result, the large and negative $-\Sigma_{10}$ term becomes dominant in $E_{\rm SW}^*(k)$. Note that even without knowing analytic expressions for Σ_{00}^* or $V_{\mathrm{QE}_R^*\mathrm{QH}f}(k)$, the fact that $V_{\mathrm{QE}_R^*\mathrm{QH}}(\infty)=0$ allows the estimate of $V_{\mathrm{QE}_R^*\mathrm{QH}}(k)$, as shown in Fig. 1(b), and of $\Sigma_{00}^*\approx 0.17\ E_{\rm C}$. Note that $V_{\mathrm{QE}_R^*\mathrm{QH}}(0)\approx -0.11\ E_{\rm C}\approx\frac{1}{6}V_{e*h}(0)$ and $\Sigma_{00}^*\approx\frac{1}{7}\Sigma_{00}$.

The dependence of the GS energy on $\zeta=K/N$ for $\nu=\frac{4}{3}$ is shown in Fig. 5(a). As in Fig. 3, ε is set to the value ε_0 for which the P and F configurations (at $\zeta=0$ and 1) are degenerate. Clearly, (almost) all energies at $0<\zeta<1$ are negative. This effect does not depend on N; on the contrary, all data points for moderate values of ζ seem to to fall on the same curve, characteristic of an infinite (planar) system. Negative excitation energies imply that the paramagnetic Laughlin $\nu=\frac{4}{3}$ state is unstable toward flipping of only a fraction $\zeta<1$ of spins when ε is decreased. This is illustrated in Fig. 5(b) where we display the data for $N=8$ corresponding to five different values of ε. The gradual decrease of ε from ε_P to ε_F drives the system through entire series of GS's (open circles) with fractional values of ζ. This sequence of GS's are distinctly different from the abrupt $P\rightarrow F$ QPT found at $\nu=2$, and they are not expected in the MFA.

We do not know the scaling of energies in Fig. 5(a) with N for large systems, but expect it to be sublinear. This implies collapse of the transition range $\Delta\varepsilon$ for $N\rightarrow\infty$, and precludes detection of the gradual $P\rightarrow F$ QPT in an infinite 2DEG. However, this QPT could still be observed in finite-size FQH droplets,[7] where $\Delta\varepsilon$ remains finite.

In conclusion, our numerical study of small systems at $\nu=2$ serves as a test of the MFA which predicts an abrupt interaction-induced $P\rightarrow F$ QPT associated with the spin-flip instability. This test should also be applicable to a similar instability and QPT which occurs for a bilayer[18] (where $\hbar\omega_c$ is replaced by the symmetric-antisymmetric splitting $\Delta_{\rm SAS}$). For the fractional $\nu=\frac{4}{3}$ state the series of spin-flip GS's between the para- and ferromagnetic states is a prediction that is susceptible to experimental observation.

The authors acknowledge partial support by the Materials Research Program of Basic Energy Sciences, US Department of Energy, and thank I. Szlufarska and G. Giuliani for helpful discussions.

[1] *The Quantum Hall Effect*, edited by R.E. Prange and S.M. Girvin (Springer-Verlag, New York, 1987).
[2] C. Kallin and B.I. Halperin, Phys. Rev. B **30**, 5655 (1984).
[3] G.F. Giuliani and J.J. Quinn, Solid State Commun. **54**, 1013 (1984); Phys. Rev. B **31**, 6228 (1985).
[4] S. Koch *et al.*, Phys. Rev. B **47**, 4048 (1993); A.J. Daneshvar *et al.*, Phys. Rev. Lett. **79**, 4449 (1997); P.T. Coleridge *et al.*, Solid State Commun. **102**, 755 (1997).
[5] D.H. Lee and C.L. Kane, Phys. Rev. Lett. **64**, 1313 (1990); S.L. Sondhi *et al.*, Phys. Rev. B **47**, 16 419 (1993); S.E. Barrett *et al.*, Phys. Rev. Lett. **74**, 5112 (1995); A.H. MacDonald *et al.*, *ibid.* **76**, 2153 (1996).
[6] A. Wójs and J.J. Quinn, cond-mat/0109548 (unpublished).
[7] O. Klein *et al.*, Phys. Rev. Lett. **74**, 785 (1995).
[8] I. Szlufarska, A. Wójs, and J.J. Quinn, Phys. Rev. B **64**, 165318 (2001).
[9] F.D.M. Haldane, Phys. Rev. Lett. **51**, 605 (1983).
[10] F.D.M. Haldane, in *The Quantum Hall Effect* (Ref. 1), Chap. 8, p. 303.
[11] A. Wójs and J.J. Quinn, Physica E **3**, 181 (1998).
[12] J.K. Jain, Phys. Rev. Lett. **63**, 199 (1989); X.M. Chen and J.J. Quinn, Solid State Commun. **92**, 865 (1996).
[13] E.H. Rezayi, Phys. Rev. B **36**, 5454 (1987).
[14] J.J. Quinn and A. Wójs, J. Phys.: Condens. Matter **12**, R265 (2000); A. Wójs and J.J. Quinn, Philos. Mag. B **80**, 1405 (2000).
[15] A. Wójs, Phys. Rev. B **63**, 125312 (2001).
[16] A. Wójs, I. Szlufarska, K.S. Yi, and J.J. Quinn, Phys. Rev. B **60**, R11 273 (1999).
[17] G. Moore and N. Read, Nucl. Phys. B **360**, 362 (1991).
[18] S. Das Sarma and P.I. Tamborenea, Phys. Rev. Lett. **73**, 1971 (1994); L. Brey, *ibid.* **81**, 4692 (1998); D.C. Marinescu, J.J. Quinn, and G.F. Giuliani, Phys. Rev. B **61**, 7245 (2000).